

High-resolution fiber-coupled spectrograph of the Hobby-Eberly Telescope

Robert G. Tull^a

McDonald Observatory, The University of Texas at Austin
Robert Lee Moore Hall 15.308, Austin, TX 78712

ABSTRACT

A high-resolution spectrograph (HRS) is taking shape for the Hobby-Eberly Telescope (HET). HRS will be mounted on a Newport bench in an insulated chamber in the "basement" of the HET building, internal to the pier, and will be linked to the corrected prime focus of the HET through its Fiber Instrument Feed. Spectra will be recorded on a 4096×4096 Orbit CCD mosaic at resolving powers of 30,000 to 120,000, using a mosaic of two R-4 echelle gratings replicated on a single blank at Spectronic Instruments and a selection of two cross-dispersing gratings. This paper will describe the design and report on the current construction status, and will describe innovative aspects, in particular a new all-refractive camera designed by Epps. The HRS design incorporates Barranne's white-pupil concept as adapted for ESO's VLT by Delabre and Dekker. Predicted performance from ray-trace analysis will be demonstrated.

With the 316-gr/mm cross-disperser the full 420-1,100 nm spectral range can be recorded in two exposures at any resolving power up to 120,000. Greater order separation can be had with the 600-gr/mm grating, requiring four exposures if the full range is needed. Designed for remote, queue-scheduled operation, HRS will be capable of rapid response to discoveries of transient phenomena. It will be directed toward discoveries of extra-solar planetary systems and studies of long-period variable stars and absorption line systems in QSOs as well as stellar nucleosynthesis and chemical compositions.

Keywords: Astronomical instrumentation, spectrographs, high resolution

1. INTRODUCTION

The Hobby-Eberly Telescope was dedicated Oct. 8, 1997 and is now proceeding toward full operational status¹. HET is a collaborative project involving the Universities of Texas, Penn State, and Stanford in the United States, Ludwig-Maximilians Universität in München and Georg-August Universität in Göttingen, Germany. Eighty of the 91 primary mirror segments, a temporary diamond-milled two-mirror spherical aberration corrector, the field acquisition camera, the primary mirror segment alignment interferometer, a fiber cable, and a fiber-fed test spectrograph were all in place at this writing in February 1998. First-light spectra have been obtained. Three permanent spectrographs are under construction. This paper will describe the high-resolution spectrograph HRS.

2. SCIENCE

HET was conceived as a spectroscopic survey telescope² to map the distribution of galaxies and quasars and to monitor G-M stars for solar-like activity. Recent discoveries of extra-solar planets (e.g. Cochran *et al.*³), the first in history, have led to a high level of expectancy for continued discovery, and the instrumental properties needed for the Search for Extra-Solar System Planets⁴ have been analyzed for application to HET⁵. High-resolution spectroscopy is the primary tool for studies of stellar nucleosynthesis. HET will permit extension of high-resolution spectroscopy to large samples of previously unreachable stars in order to obtain critical insight to the formation and early stages of evolution of the stellar population of the Galaxy⁶. High spectral resolution, broad spectral coverage at high efficiency, a very large telescope aperture, and wavelength stability are prime requirements for many of these programs.

Further author information -

^a R.G.T. (correspondence): Email: rgt@astro.as.utexas.edu; Telephone: 512-471-3328; Fax: 512-471-6016

3. INSTRUMENTAL REQUIREMENTS

Technical specifications for HRS were designed to meet the needs of proposed and future research involving high-resolution survey spectroscopy. In survey work, spectra of faint objects scattered over the whole sky have to be obtained in the shortest possible exposure times (thus the demand for a very large telescope) and the instrument has to be capable of rapid set-up on succeeding objects. The process of establishing the design specifications has been iterative, depending not only on the science needs but also on the realities of optical design and of funding opportunities.

For the vast majority of stars within reach of high-resolution spectrometry, atmospheric temperatures range from 25,000 K $\geq T_{\text{eff}} \geq 4,000$ K. Full analysis of their absorption spectra requires that the resolving power be in the corresponding range $20,000 \leq (R = \lambda/d\lambda) \leq 120,000$. Sneden⁷ summarized the arguments from which we established a primary HRS requirement $R = 60,000$. With modern advances in CCD and diffraction grating technology it has now become practical to achieve $R = 120,000$ with full spectral coverage in one or, at most, a few exposures and we made this a secondary goal. The primary goal is to be achieved with optical fibers of diameter > 1 arcsec, to maximize transmission in the presence of real, seeing-limited star images. Efficient high-resolution spectroscopy proves elusive on a large telescope with current technology and image slicers are necessary. With first-order gratings to separate echelle spectral orders the maximum spectral pass-band that can be obtained in a single exposure is limited by overlapping orders to one octave (factor of two) of wavelength coverage; that became the specification for single exposures. The overall pass-band is 420 nm - 1.1 μm . Simultaneous acquisition of the entire pass-band was an original goal; this was discarded when funding for a two-channel spectrograph was not forthcoming. The blue limit is imposed by the predicted throughput efficiency of the HET with its over-coated silver (FSS-99) mirrors and fiber optics, and the red limit is the near-IR cutoff of silicon CCDs.

Figure 1 shows the calculated spectral efficiency of the telescope in 1-arcsecond seeing with a 1.5" optical fiber of 35-m length⁸, excluding HRS but multiplied by the expected spectral sensitivity of the CCD detector. This effectively defines the HRS spectral band-pass. From this calculation plus the expected throughput of the HRS we can calculate the limiting magnitudes at $R = 60,000$. With one arc-second seeing and a fiber of diameter 1.8", we predict a 1-hour exposure will reach stellar magnitude $V = 14.4$ at $S/N = 100$ or $V = 19.4$ at $S/N = 10$. The predicted peak transmittance of the telescope - spectrograph combination, including the detector, is 15%.

A mosaic of two CCDs manufactured in the Orbit Semiconductor, Inc. wafer fabrication facility serves as the spectral image detector. Each has $4,096 \times 2,048$ 15- μm square pixels. The longest HRS spectral orders in the near-IR are matched to the full width of the detector by a camera with 500-mm focal length, with the 31.6-gr/mm R-4 echelle. The spectral resolution element at $R = 60,000$ is four pixels. This allowed us the secondary goal of resolving power $R = 120,000$ in the limit with two-pixel resolution.

Spectral orders are separated by cross-dispersion and are simultaneously recorded on the large-area CCD. The use of prisms was found impractical on such a large telescope with current technology and we adopted first-order diffraction gratings for order separation. The separation needed for accurate determination of the scattered light, including background skylight, led to the choice of two gratings, which are interchangeable as needed. For detection of extra-solar-system planets, wavelength

stability better than 10 m/s over an observing session has been an important consideration in setting the specifications for HRS. A quarter century of experience with the McDonald Observatory coude spectrographs has served well as a role model in developing a spectrograph that will achieve stability through strict adherence to kinematic design principles and judicious use of pupil stops.

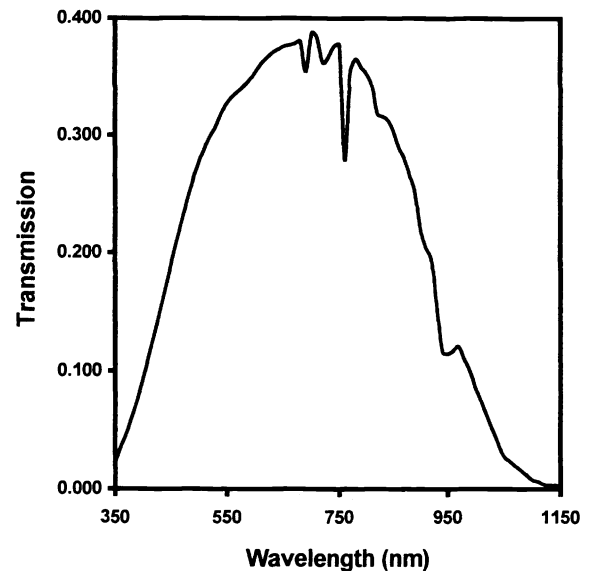


Figure 1. Predicted transmission of the atmosphere, HET, 35-m 1.5-arcsecond fiber, and CCD in 1" seeing.

An atmospheric dispersion compensator is to be included in the prime focus assembly, to assure maximum throughput efficiency of the fiber feed and maximum stability of the recorded spectral energy distribution. Because focal ratio degradation in the fiber optics will inevitably spread light into the telescope's central shadow, an all-refractive camera was specified, to avoid loss of that light due to blockage by the central obstruction common to on-axis reflective cameras.

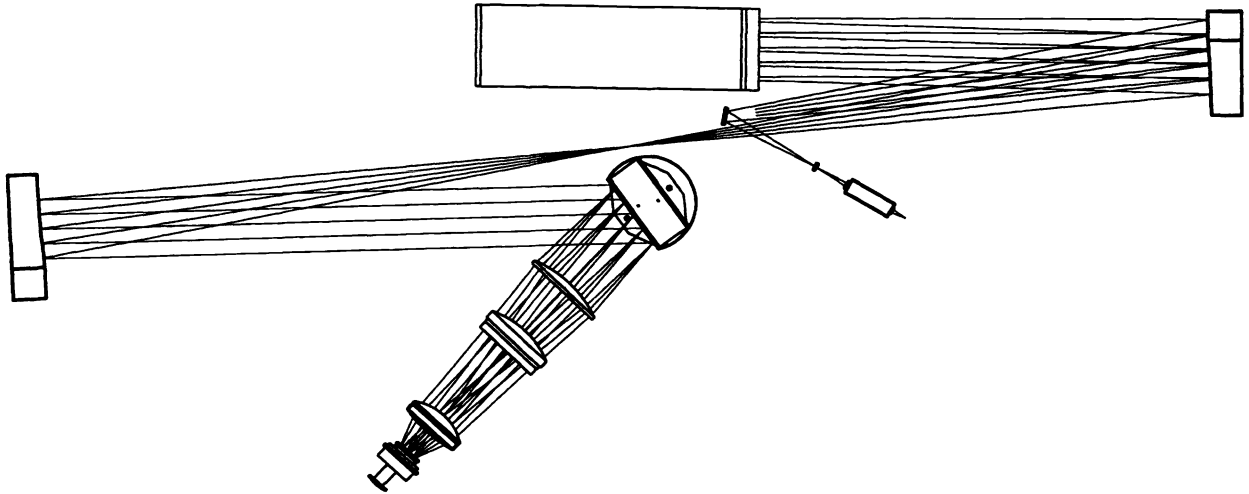


Figure 2. Plan view, HET High Resolution Spectrograph (HRS).

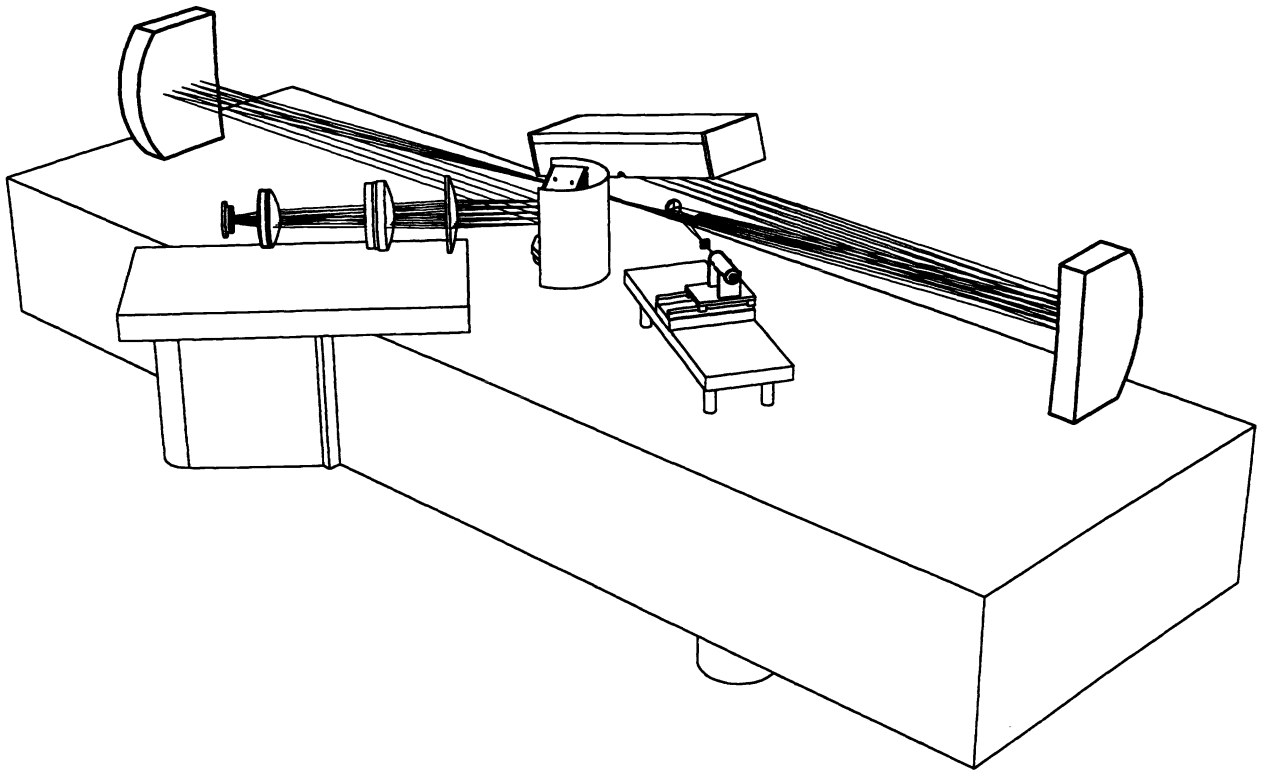


Figure 3. Perspective view.

4. SPECTROGRAPH DESIGN THEORY

Schroeder⁹ gave the basic equations for the “luminosity” of a seeing-limited slit spectrograph. He showed a reduction of overall efficiency with increasing departure θ from the Littrow condition. In an earlier paper¹⁰ I showed that, in the Littrow configuration, the luminosity could be given in the form

$$R \times \phi = 2 \sin \theta_B \times \frac{L}{D_T}. \quad (1)$$

Here, $R = \frac{\lambda}{\Delta\lambda}$ is the resolving power, ϕ is the angular width of the slit projected on the sky, D_T is the telescope aperture, L is the ruled length of the echelle, and θ_B is the blaze angle of the grating. Compared with the usual form (e.g. Tull¹⁰ Equation (2)) involving the beam aperture D_C and $\tan \theta_B$, Equation (1) more clearly demonstrates the limits of spectrograph design when available echelle dimensions are limited. For an echelle of maximum available ruled length, there is only a very slow gain of throughput with increased θ_B but a rapid decrease in required beam diameter $D_C = L \cos \theta_B$. This is the critical clue to matching a high-resolution spectrograph to a very large telescope at moderate cost. For a given telescope, an R-4 echelle (i.e., a diffraction grating with $\tan \theta_B = 4.0$) permits a spectrograph design with smaller optical components without sacrifice of resolving power or slit throughput efficiency, compared to an R-2 echelle of the same length.

In Equation (1) the only free spectrograph parameters are the blaze angle θ_B and length L of the echelle grating. Line tilt, line curvature, and their variations with position in the focal plane increase with blaze angle θ_B and with the off-plane angle γ . Tasks in designing the spectrograph reduce to maximizing θ_B and L while minimizing the off-Littrow and off-plane angles θ and γ , for maximum speed and minimum spectral line tilt. The David Richardson Gratings Laboratory of Spectronic Instruments, Inc. has taken major steps in increasing θ_B and L : in 1995 they successfully replicated a mosaic of two R-4 echelles onto a single blank, with 31.6 grooves/mm over a total ruled area of 211×836 mm, under contract with ESO^{11,12}. This doubled the length *and* the tangent of the blaze angle, compared to the most widely used echelles previously available. Use of any grating at a blaze angle as great as 75° is complicated by the need to minimize θ . The ESO design of the UVES spectrograph for the VLT¹³, which uses the first collimator mirror in double pass, provided a powerful solution to this problem and many aspects of that design were adopted for HRS.

5. DESCRIPTION AND STATUS OF HRS

The optical design is a single-channel adaptation of the ESO UVES spectrograph^{10,13,14}. It uses an R-4 echelle mosaic in the quasi-Littrow mode for maximum possible efficiency, with cross-dispersing gratings to separate spectral orders. An all-refracting camera feeds the image to a large-area mosaic CCD. Residual field curvature and astigmatism are reduced at the camera focus by a field flattener lens, one surface of which has a cylindrical figure. We adopt the “white pupil” spectrograph concept of Baranne¹⁵ to further maximize efficiency and optical performance while minimizing cost. Departures from the UVES design are

- (a) The HRS is a single-channel spectrograph.
- (b) The HRS is not folded, saving one reflection.
- (c) The camera was re-designed to match the selected image detector and to minimize vignetting.
- (d) The pre-slit area is designed to accommodate an optical-fiber interface and image slicers.

The design and performance parameters for the spectrograph are listed in Tables 1 and 2; the design is illustrated in Figures 2 and 3. The spectrograph is linked by optical fibers from the HET prime focus 4-mirror spherical aberration corrector, which delivers an $f/4.58$ beam to the fiber optic feed at an image scale of 4.889 arcseconds/mm. At the spectrograph end of the fiber the focal ratio is converted to $f/10$, with an image of the fiber ends illuminating the spectrograph slit. Interchangeable image slicers and slits will maximize efficiency at the user-selected resolving power. The design is optimized for operation over the pass-band $420 \text{ nm} - 1.1 \text{ }\mu\text{m}$ at spectral resolving powers $30,000 \leq R \leq 120,000$. Interchangeable cross-dispersing gratings permit a selection of two format configurations at the CCD, one producing the maximum possible spectral pass-band and the other with increased order separation for inclusion of background sky spectra.

Table 1.

HRS Design Parameters					
ELEMENT		Size	Blaze angle, etc.	Effective Blaze λ	
R-4 Echelle		31.6 gr/mm	210x836	75.07°	"all"
Cross-Dispersing Grating	#1	316 gr/mm	204x254 mm	6.80°	610 nm m = 1
Cross-Dispersing Grating	#2	600 gr/mm	220x250 mm	approx. 10°	510 nm m=1
Collimator (off-axis parab.)	M1	f=2 m f/10	540x350 mm		
Collimator (off-axis parab.)	M2	f=2 m f/10	540x250 mm		
Refractive Camera		f= 0.5 m f/1.9	Aperture 28 cm	Field 88 mm	Pass-band 420-1100 nm
Star Fiber diameters	#1	1.5"		300 μ m	
	#2	3.0"		600 μ m	
Image Dissectors	#1	(7-Fiber Bundles)	fiber diameters	100 μ m	
	#2			200 μ m	
Image Detector	2 x (2048 x 4096 x15- μ m) pixels Orbit CCD Array				

Table 2.

HRS Performance Parameters						
R x ϕ	34,000"					
Effective Slitwidth	1.12"	0.56"	0.28"			
	500 μ m	250 μ m	125 μ m			
Resolving Power	8.3 pixels	4.2 pixels	2.1 pixels			
	30,000	60,000	120,000			
X-Grating	#1 (316 gr/mm)			#2 (600 gr/mm)		
Order Separation @ λ	4.4" @ 420 nm	12" @ 700 nm	31" @ 1.1 μ m	8.2" @ 420 nm	22" @ 700 nm	45" @ 1.0 μ m
Spectral Coverage per CCD height	420-790 nm	570-940 nm	740-1110 nm	420-620 nm	620-820 nm	820-1020 nm

The theory of the two-mirror collimator system has previously been described^{10,13}. The first off-axis paraboloidal mirror M_1 works in double-pass, focussing the spectrum at an intermediate focus where it passes through a stray-light baffle. This permits quasi-Littrow use of the echelle with $\theta = 0.0^\circ$ and $\gamma = 0.8^\circ$, for maximum possible efficiency. A second, identical mirror M_2 re-collimates the light, canceling the off-axis astigmatism of M_1 and projecting the white pupil image of the echelle onto the cross disperser.

Figuring of the collimator mirrors is under contract to Don Loomis of Custom Optics in Tucson, AZ. Mirror M_1 has been completed and is at Denton Vacuum for FSS-99 silver coating. The 316 gr/mm cross-dispersing grating is in hand and the master for the 600 gr/mm grating is now being ruled; both are Spectronic Instruments, Inc. grating replicas.

6. R-4 MOSAIC ECHELLE

The echelle grating was received from Spectronic Instruments, Inc. in June 1997. It is a mosaic of two 31.6 gr/mm echelles replicated on a single Zerodur blank of dimensions $214 \times 840 \times 125$ mm. The ruled area is 210×836 mm with a 14-mm gap between the two replicas. The blaze angle is 75.07° , making this nominal R-4 echelle a true R-3.75 echelle. This cosmetically beautiful grating passed all tests in the David Richardson Gratings Lab.

Figure 4, derived from the test report, illustrates the resolving power of the echelle at the wavelength of a single-mode HeNe laser using a 10-m focal length test camera. The echelle was illuminated with an 8-inch collimated beam and the entrance and exit slits were almost closed (10–30 μm width). The exit slit was scanned across the image. The horizontal unit in Figure 4 is one inch on the resulting chart paper. The resulting line-width (FWHM) is 0.0061 \AA , corresponding to resolving power $R = 1,050,000$. For this grating the theoretical resolution of a single segment is 1.2 million at 6328 \AA , and the resolution achieved is 88% of theoretical. No attempt to phase the two segments was made or required; the resolving power requirement is fully achieved without phasing. It should be pointed out that the resolving power of the identical ESO echelle is 2 million. It appears, then, that phasing is in fact possible but this was not a controlled parameter. In any case, the achieved resolving power is nearly an order of magnitude greater than required for HRS.

In additional tests the echelle was illuminated with a mercury source. Five central components of the mercury hyperfine structure were visible in the 5461 \AA line in 112th order, confirming resolution of at least 900,000. An interferogram obtained with a 6-inch beam shows a relative wavefront tilt between the two segments amounting to 2 fringes of 6328- \AA light over half the aperture, equivalent to 3.5 arcseconds. For HRS on the HET, with a 9.21-m aperture, the resulting image error at the camera focus is equivalent to an effective wavefront error less than 0.1 arcseconds projected on the sky. In wavelength space, the 3.5" error would result in a doubled image with separation 8.5 μm in the focal plane of the HRS camera, about one pixel, or 0.014 \AA at 6328 \AA . That might be expected to degrade the resolution to about 440,000, still far greater than needed for HRS. However, such degradation is not observed in Figure 4 unless it

accounts for the minor image doubling present. Grating ghosts are present, as seen in Figure 5 (reproduced from the test report), with maxima of 6×10^{-5} of the parent line, just 2/3 the intensities seen in our best R-2 echelle at the 2.7-m 2dcoudé spectrograph.

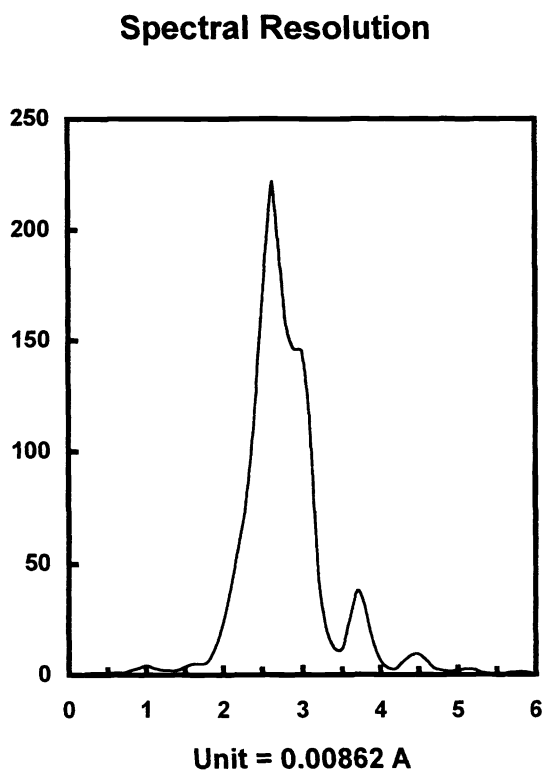


Figure 4. Instrumental profile for the R-4 echelle at the focus of a 10-m test bench at Spectronic Instruments.

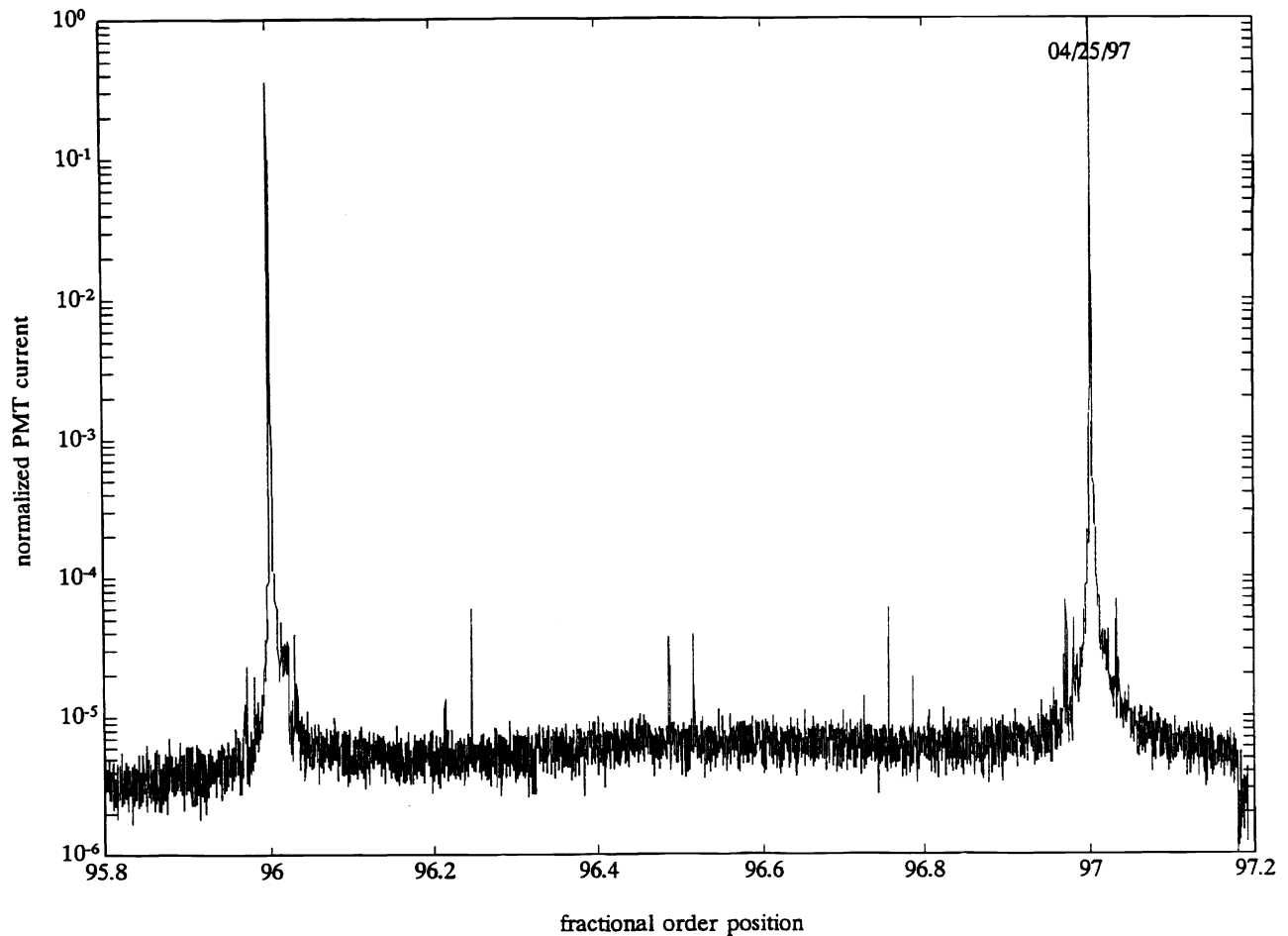


Figure 5. Scan of the R-4 echelle between the 96th and 97th orders of the HeNe laser line at 632.8 nm. This figure is reproduced from the Spectronic Instruments, Inc. test report.

As in the ESO UVES, two first-order gratings are mounted back-to-back on a rotary stage with vertical rotation axis. These serve as the cross dispersers. Either grating is selected by a 180° rotation, while fine motion about the same rotation axis centers the desired echelle order on the CCD. For the selected echelle, camera, and CCD all order lengths fit within the borders of the CCD up to wavelength 960 nm. Optional use of smaller CCDs and avoidance of bad pixels or columns will require the ability to re-position spectra in both x and y . For ultimate stability we designed a three-position tilt mechanism permitting rotation of the echelle in discrete 1° steps. Similarly, the two-grating cross-disperser turret will be rotated in nine discrete steps at intervals of one and two degrees for the 316 and 600 gr/mm gratings, respectively. Order separation is 4.4 arc-seconds at 420 nm, increasing to 26 arc-seconds at 1.04 μm , with the 316 gr/mm cross disperser. The master for a second first-order grating with 600 gr/mm with effective blaze around 5500 Å is currently being ruled at the Richardson Gratings Lab. This grating will provide nearly double the order separations of the 316 gr/mm grating.

7. CAMERA

The camera is an Epps design¹⁶. Most of the optical glass is on hand and Coastal Optical Systems Inc. has been contracted to do the optical shop processing. Epps optimized the design for the full spectral band-pass permitted by the over-coated silver mirrors used throughout the HET and HRS and by the CCD spectral sensitivity and fiber-optics transmittance (see Figure 1). A 260 mm diameter entrance pupil is coincident with the HRS white pupil and the cross-dispersing grating, and lies 330 mm

in front of the first lens element. That lens has an aperture 280 mm, the largest of the eight. With its focal length of 500 mm, the camera focal ratio is $f/1.92$ to accommodate nearly the full diagonal of the diffraction gratings. The camera's 88-mm diameter focal surface is flat. We expect completion of the optical work in September 1998.

From ray tracing analysis of the full HRS, there is a residual cylindrical field curvature at the camera focus. Radii of curvature of the field are -1.19 m in x (convex toward the camera lenses, along the direction of echelle dispersion) and $+14$ m in y . In the y axis, longitudinal astigmatism is negligible, varying from 0.02 mm at the center of the field to .04 mm in the reddest and bluest spectral orders. Along the spectral orders, astigmatism increases to 0.4 mm near the edges of the field. The cylindrical field curvature can be understood in terms of classical optics by the following argument:

The field curvature and astigmatism of a mirror can be calculated from equations given by Gascoigne¹⁷: for a paraboloidal mirror of focal length f with aperture stop at distance d , the aberration coefficients C and D are

$$C = \frac{1}{2f} - \frac{d}{2f^2}, D = C - \frac{1}{2f} \quad (2)$$

and the longitudinal astigmatism and field curvature are $2Cf^2\phi^2$ and $-2C + 2D$. When the stop is in the focal plane, $d = f$ and astigmatism $C = 0$. In this case, which corresponds to HRS collimator mirror M1 in the plane of echelle dispersion, field curvature at the intermediate focus is that of the Petzval surface and is $2D$. From Equations 2, $2D = -1/f$ and the radius of curvature is -2 m. Gascoigne's sign convention means it is convex to the incident light. Ray tracing shows the radius of curvature at this focus to be -2.1 m, in close agreement with theory.

In the perpendicular plane (the plane of the drawing Figure 2), light from the echelle falls on M1 at angle $\phi = 2\gamma = 1.6^\circ$, with the echelle offset 285 mm. Projecting that beam through the first collimator mirror M1 to its intersection with the optic axis gives the distance to an effective stop at $d = -8.2$ m; the theoretical longitudinal astigmatism is $2Cf^2\phi^2 = 7.95$ mm. In this plane the field width is zero. Ray tracing shows longitudinal astigmatism = 7.93 mm, again in close agreement with theory. Ray tracing further shows that the astigmatism due to the off-axis paraboloid M1 is effectively compensated by mirror M2. Because field width perpendicular to echelle dispersion is due entirely to the cross dispersing grating, which lies in the white pupil and is coincident with the camera pupil, the field curvature in that dimension is that of the Epps camera alone, which is flat. The resulting cylindrical field curvature due to the overall HRS has been partially compensated by a convex cylindrical figure formed on the last camera surface. When we attempted complete compensation, some image degradation occurred on the best flat focal surface at the edge of the field, and we accepted a minor compromise to achieve best overall performance.

Figures 6 and 7 show spot diagrams on a flat focal surface in the red and blue ranges, with the 316-gr/mm cross grating. The boxes are 4×4 pixels. For the computations that led to Figures 8 and 9, the input source had a Gaussian intensity distribution over-filling slit-widths corresponding to resolving powers 60,000 and 120,000. The FWHMs of the intensity cross-sections of the ray-traced images were used to calculate resolving power along several spectral orders across the focal plane. These show that slit-limited resolving power as high as 120,000 is in fact achievable, given excellent-quality optics.

A mosaic of two Orbit CCDs, each with 2048×4096 15- μ m pixels, serves as the image detector. The individual CCDs are butttable on three edges. Orbit Semiconductor, Inc. produced these chips under a cooperative arrangement between the Lick and McDonald Observatories. At this writing the chips are awaiting processing in the CCD thinning lab at Steward Observatory.

8. CONCLUSION

This paper describes the principal characteristics of a single-channel, fiber-linked high-resolution spectrograph (HRS) for the Hobby-Eberly Telescope. Changes from the prototype ESO UVES design include elimination of a folding flat, inclusion of a fiber feed with interchangeable image slicers and slits, and a new refractive camera design by Epps. HRS is mounted on a standard off-the-shelf optical bench and housed in an insulated chamber inside the telescope pier at the end of a 35-m fiber-optic cable. It is scheduled for completion and installation during the first quarter of 1999.

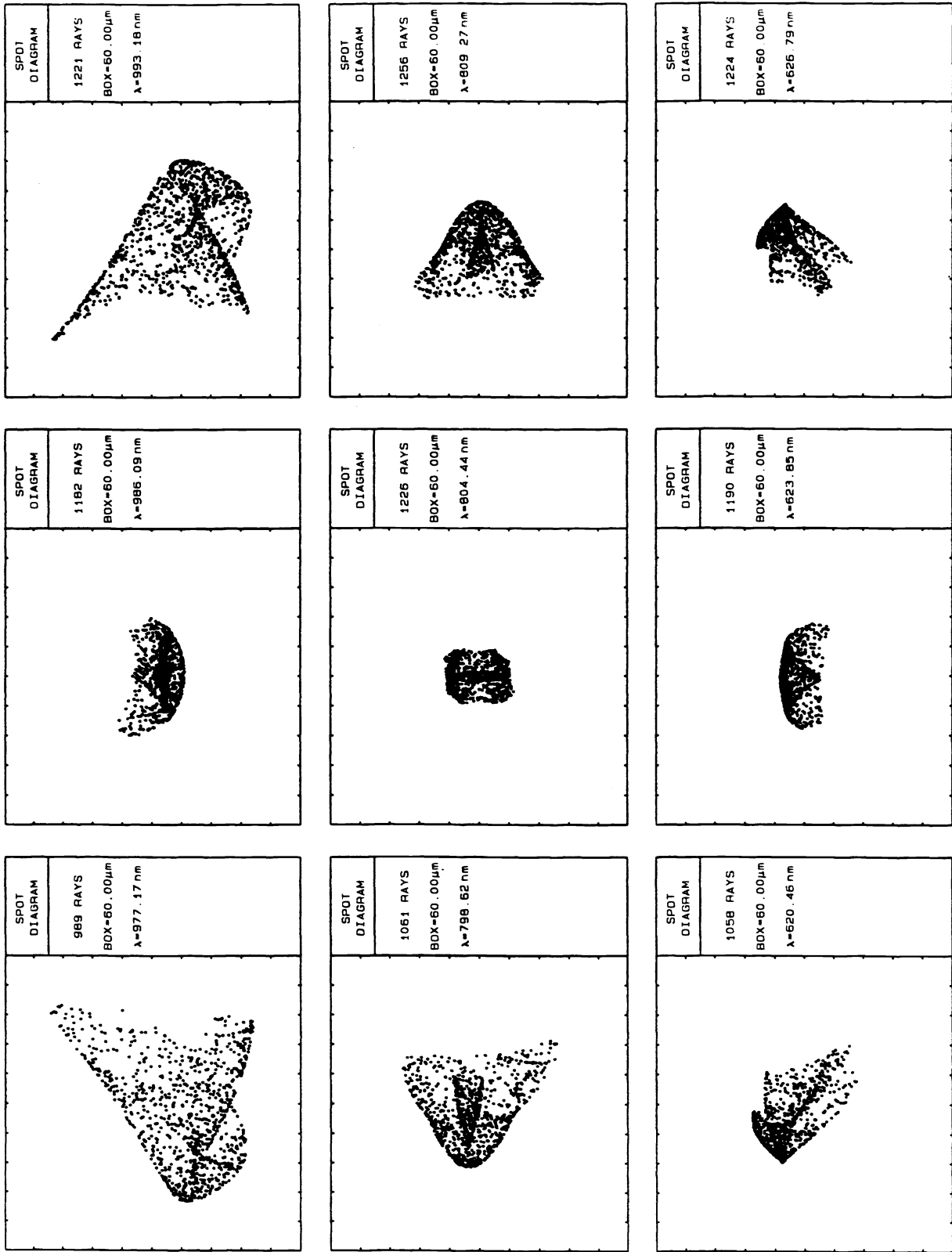


Figure 6. Ray-traced spot diagrams for a point source, for the full HRS with Epps camera, in a "best" flat focal surface. Red range.

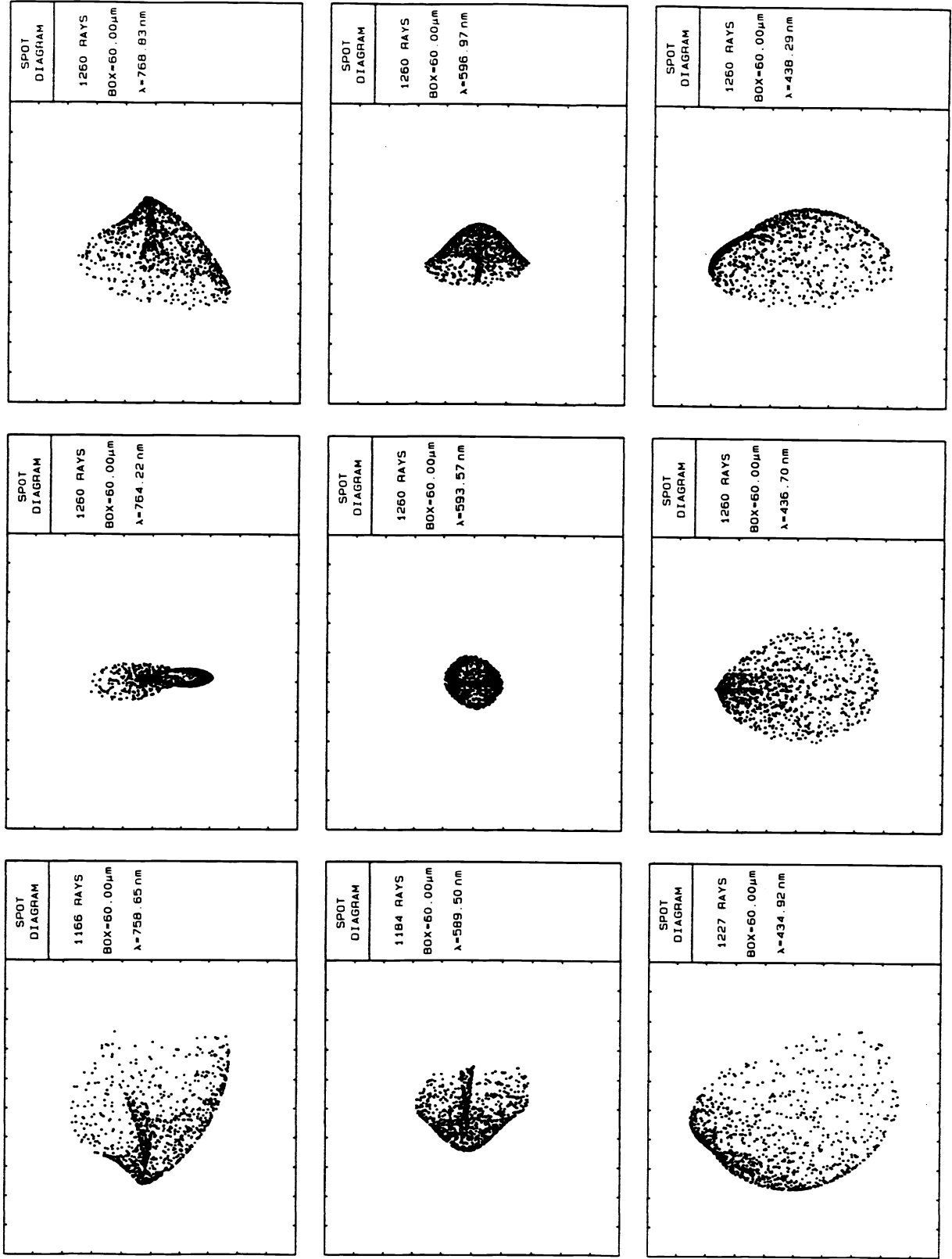


Figure 7. Ray-traced spot diagrams for a point source, for the full HRS with Epps camera, in a "best" flat focal surface. Blue range.

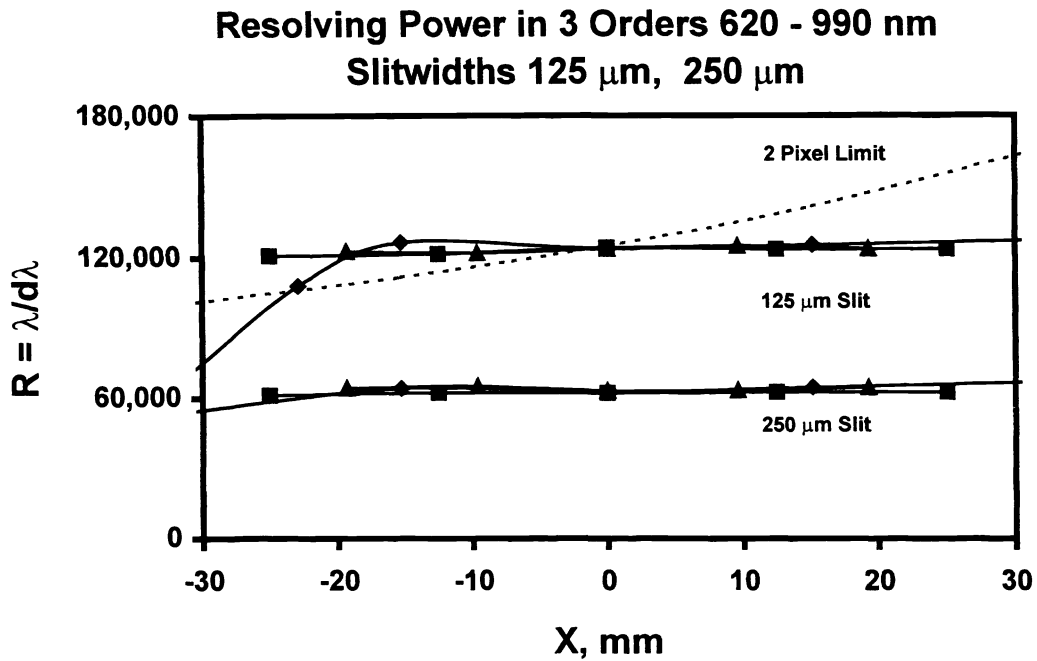


Figure 8. Resolving power computed from ray traces in three spectral orders in the HRS red range. These spectra lie across the center, the top edge, and the bottom edge of the camera field. Whereas the spectral dispersion varies with dispersion angle along each order, so do the widths of the slit image projected on the CCD so that R is nearly constant across the field except for instrumental aberrations. Cases shown are for two slit-widths corresponding to $R = 60,000$ and $R = 120,000$.

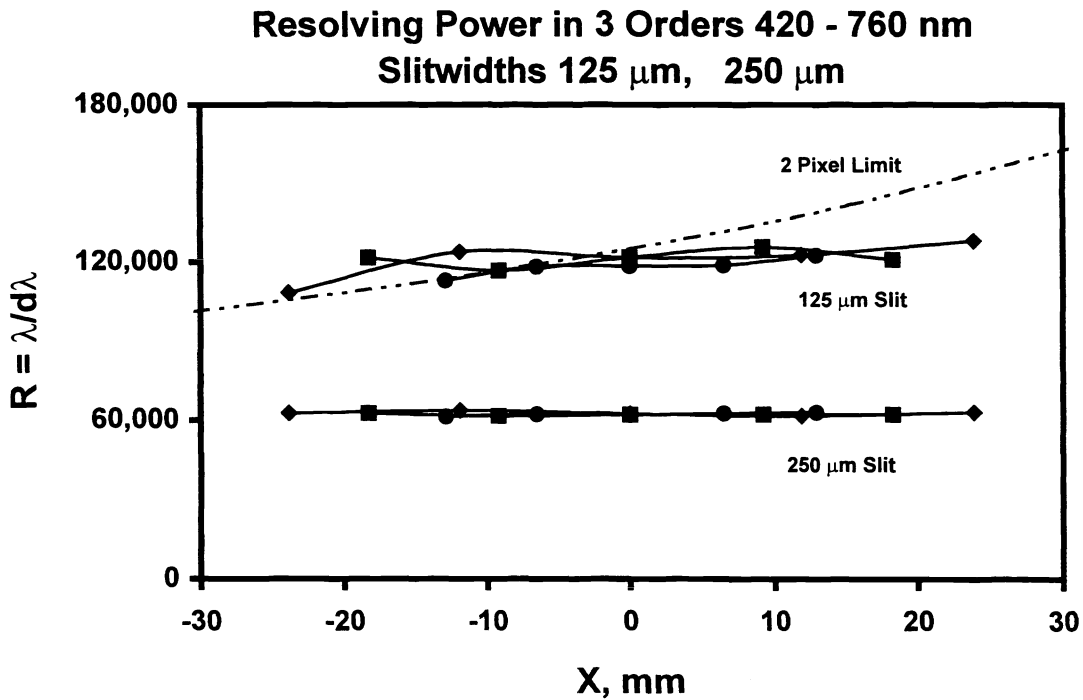


Figure 9. Same as in Figure 8 but the cross-dispersing grating has been tilted to expose the HRS blue range.

9. ACKNOWLEDGEMENTS

Many useful discussions with ESO's Hans Dekker, with Thomas Gehren and Michael Pfeiffer of the Universitäts-Sternwarte München, and with John Booth of the University of Texas have contributed to the final design concept. The HRS project team has included Don Barry, Artie Hatzes, Bill Cochran, David Lambert, Phillip MacQueen, and Chris Sneden, all of the University of Texas, and Larry Ramsey of Pennsylvania State University. John Good is chief mechanical engineer and Phillip MacQueen is in charge of detector development. The author gratefully acknowledges generous support from the National Science Foundation, the National Aeronautics and Space Administration, and the State of Texas. Additional support was kindly provided by gifts from the McDonald Observatory and Department of Astronomy Board of Visitors and from Ben and Mary Anderson, and by a memorial gift honoring Mrs. Oveta Culp Hobby. McDonald Observatory provided partial salary support and The University of Texas Administration contributed matching funds.

10. REFERENCES

- ¹ Ramsey, L. W., Adams, M. T., Barnes, T. G. III, Booth, J. A., Cornell, M. E., Gaffney, N. I., Glaspey, J. W., Good, J. M., Fowler, J. R., Kelton, P. W., Krabbendam, V. L., Long, L., Ray, F. B., Ricklefs, R. L., Sage, J., Sebring, T. A., Spiesman, W. J., Steiner, M., "Early performance and present status of the Hobby-Eberly Telescope," in *Advanced Technology Optical/IR Telescopes VI*, Proc. SPIE Conf. 3352, paper 06, 1998.
- ² Ramsey, L., and Weedman, D. W., "The Penn State Spectroscopic Survey Telescope," in *Very Large Telescopes, their Instrumentation and Programs*, IAU Colloq. 79, ed. M.-H. Ulrich and K. Kjær, pp. 851-860, 1984.
- ³ Cochran, W. D., Hatzes, A. P., Butler, R. P., Marcy, G. W., "The Discovery of a Planetary Companion to 16 Cygni B", *Astrophys. J.* **483**, pp. 457-463, 1997.
- ⁴ Cochran, W., and Hatzes, A., "A High Precision Radial-Velocity Survey for Other Planetary Systems," *Astrophys. & Space Sci* **212**, pp. 281-291, 1994.
- ⁵ Hatzes, A. P., and Cochran, W., "Spectrograph Requirements for Precise Radial Velocity Measurements," in *Proc. ESO Workshop on High Resolution Spectroscopy with the VLT*, ed. M.-H. Ulrich, pp. 275-278, 1992.
- ⁶ Lambert, D. L., in *Cosmic Abundances of Matter*, AIP Conf. Proc. **183**, ed. J. P. Waddington, New York, Am. Inst. Phys., p. 168, 1989.
- ⁷ Sneden, C., "Report of the High Resolution Spectroscopy Working Group," in *The Spectroscopic Survey Telescope*, Proc. of a Workshop at Penn State University, ed. F. Cordova, pp. 71-75, 1990.
- ⁸ Ramsey, L. W., HET internal report "Fiber Instrument Feed Critical Design Review," Pennsylvania State University, Dec. 18, 1997.
- ⁹ Schroeder, D., *Astronomical Optics*, Academic Press, 1987.
- ¹⁰ Tull, R. G., "High resolution spectrograph for the spectroscopic survey telescope", in *Instrumentation in Astronomy VIII*, Proc. SPIE Conf. **2198**, ed. D. L. Crawford, pp. 674-685, 1994.
- ¹¹ Test report, "ESO Mosaic Project, Test results of 31.6 gr/mm R-4 red echelle mosaic," Milton Roy Co. March 31, 1995.
- ¹² Dekker, H., and Hoose, J., "Very High Blaze Angle (R-4) Echelle Mosaic," in *ESO Workshop on High Resolution Spectroscopy with the VLT*, ed. M-H Ulrich, 1992.
- ¹³ Delabre, B., "ESO - Very Large Telescope: UVES preliminary optical design report," ESO Internal Doc. No. VLT-TRE-ESO-13200-0272, 6 Oct. 1993.
- ¹⁴ Dekker, H., and D'Odorico, S., "UVES, the UV-Visual echelle spectrograph for the VLT," *The Messenger*, No. 70, pp. 13-17, Dec. 1992.
- ¹⁵ Barranne, A., "Equipement Spectrographique du Foyer Coudé du Telescope de 3,60 mètres, Etude de faisabilité d'un spectrographe universel," in *Auxiliary Instrumentation for Large Telescopes*, ESO/CERN Conf., ed. S. Laustsen and A. Reiz, p. 227, 1992.
- ¹⁶ Epps, H. W., "Development of large high-performance lenses for astronomical spectrographs," in *Optical Astronomical Instrumentation*, Proc. SPIE Conf. **3355**, paper 64, 1998.
- ¹⁷ Gascoigne, S. C. B., "Recent Advances in Astronomical Optics," *Appl. Opt.*, **12**, p. 1419, 1973.